

# Sensitivity of stellar physics to the equation of state

D.C. Swift, T. Lockard, M. Bethkenhagen,<sup>1</sup>A. Kritcher, S. Hamel,  
and  
D. Dearborn

*Lawrence Livermore National Laboratory, 7000 East Avenue, Livermore, California 94550, U.S.A.*

March 2, 2019; updates to June 28, 2020

## ABSTRACT

The formation and evolution of stars depends on various physical aspects of stellar matter, including the equation of state (EOS) and transport properties. Although often dismissed as ‘ideal gas-like’ and therefore simple, states occurring in stellar matter are dense plasmas, and the EOS has not been established precisely. EOS constructed using multi-physics approaches found necessary for laboratory studies of warm dense matter give significant variations in stellar regimes, and vary from the EOS commonly used in simulations of the formation and evolution of stars. We have investigated the sensitivity of such simulations to variations in the EOS, for sun-like and low-mass stars, and found a strong sensitivity of the lifetime of the Sun and of the lower luminosity limit for red dwarfs. We also found a significant sensitivity in the lower mass limit for red dwarfs. Simulations of this type are also used for other purposes in astrophysics, including the interpretation of absolute magnitude as mass, the conversion of inferred mass distribution to the initial mass function using predicted lifetimes, simulations of star formation from nebulae, simulations of galactic evolution, and the baryon census used to bound the exotic contribution to dark matter. Although many of the sensitivities of stellar physics to the EOS are large, some of the inferred astrophysical quantities are also constrained by independent measurements, although the constraints may be indirect and non-trivial. However, it may be possible to use such measurements to constrain the EOS more than presently possible by established plasma theory.

*Subject headings:* Equation of state - Stars: composition - Stars: interior

## 1. Introduction

A unique characteristic of astrophysics is the limited information about bodies observed, leading to a reliance on a network of supporting assumptions. This is even true of geophysical knowledge about the Earth, for instance because the composition of the core and mantle cannot be measured directly, and applies even more to planets and exoplanets. Assumptions are made about the composition and internal structure, using the equation of state (EOS) for relevant compositions of matter to discriminate possible from unlikely in-

terpretations. The EOS even more important for stellar structure and evolution, because, as well as guiding the interpretation of structure through compressibility, the rate of thermonuclear reactions depends sensitively on temperature.

We have developed laboratory experiments probing a wider ranges of states than were accessible previously, in particular at the National Ignition Facility (NIF) (e.g. Doeppner et al 2018; Swift et al 2018; Kritcher et al 2020; Swift et al 2020). These experiments are able to explore progressively more regimes of direct relevance to stellar structure. Such measurements also provide more constraining validation of EOS models, where consistent physics can be used between the regimes probed experimentally and those occur-

<sup>1</sup>Present address: CNRS, École Normale Supérieure de Lyon, Laboratoire de Géologie de Lyon, Centre Blaise Pascal, 46 allée d’Italie, Lyon 69364, France

ring in stars.

The purpose of work reported here is to assess the sensitivity of some key stellar structure and evolution simulations to variations in the EOS. We chose the lifetime of the Sun, and the lower mass limit of a red dwarf. The latter was a proxy for lower mass limit of a brown dwarf, which is potentially more interesting as a factor in evaluating the amount of excess gravitational binding attributable to dark matter, but the brown dwarfs are thought to be significantly more complicated to simulate than red dwarfs, as discussed below. We compare simulations of the structure and evolution of stellar bodies with variations between representative EOS. We also assess the relationship with uncertainty in the mass budget for exotic dark matter.

The sensitivities we present are raw, without adjusting other models. Coupled with the uncertainty in an EOS, the sensitivities do not imply a formal uncertainty in any particular property of a star: one would adjust other models such as the composition, opacity, and convective transport within their respective uncertainties to match observables of the star and hence re-constrain the overall model, usually reducing the effective uncertainty. However, the raw sensitivity calculated here is the more relevant representation of the sensitivity to a specific model such as the EOS. Equivalent sensitivities are used widely in other applications such as inertial confinement fusion.

Analogous studies have been reported recently of the sensitivity to opacity (Guzik et al 2018).

## 2. Stellar evolution simulations

Stellar evolution simulations are usually performed with one spatial dimension treated explicitly (the radius), for an initial condition comprising the composition and state (mass density  $\rho$  and temperature  $T$ ) as a function of radius. As the star evolves, gravitational energy and thermonuclear reactions produce heat, which is conducted and convected within the star and radiated from its surface, the composition changes via the reactions. As the simulation usually covers a long period (billions of years) compared with the characteristic oscillation time of the star (hours), the motion of stellar matter under pressure gradients is not tracked explicitly, and instead the simula-

tion proceeds by finding the instantaneous structure that is stable with respect to gravitational buoyancy.

Simulations were performed using the computer program STARS (Eggleton 1971, 1972, 1973; Eggleton et al 1973; Eldridge et al 2004; Pols et al 1995; Schroeder et al 1997; Stancliffe et al 2009, 2004, 2005, 2007). For our present purposes we are interested in the calculation of material properties, the `statef` subroutine in STARS. For comparison with alternative programs, we note the key models used for material properties. Fermi-Dirac integrals were evaluated per Eggleton et al (1973). ‘High-Z’ species were treated as completely ionized, which is unlikely to be accurate, but is probably unimportant as we focused on cases with low-Z compositions. Partition function for  $H_2$  was taken from (Vardya 1960; Webbink 1975), representing ionization and molecular dissociation. Molecular opacities were taken from (Alexander & Ferguson 1994), electronic conduction from (Itoh & Kohyama 1993), and otherwise the OPAL model was used (Iglesias et al 1992). Dissociation coefficients were taken from (Rossi & Maciel 1983). Opacities for molecular CN were from (Scalo & Ulrich 1975); CO, OH and  $H_2O$  were from (Keeley 1970; Marigo 2002). Neutrino loss rates were taken from (Itoh et al 1983, 1989, 1992).

Each simulations began with a cloud of cool gas collapsing under gravitational attraction. Nuclear reactions arrest the collapse and lead to a steadily-evolving star. (Fig. 1.)

To perform a sensitivity study, the simulations were repeated with a perturbation made to the EOS. Each perturbation was a scaling of the pressure and specific internal energy. For each case, we extracted a representative state at the center, of mass density  $\rho$ , temperature  $T$ , and composition, and compared the pressure calculated using different EOS.

## 3. Lifetime of the Sun

STARS simulations of the Sun capture its condensation, a slow evolution through its present state, and its eventual expansion as red giant. We performed simulations using the default solar model profile, which has been optimized to give the currently observed radius and luminosity. This

model is consistent with a present age of  $\sim 7$  Gyr, and predicts the formation of red giant  $\sim 5.5$  Gyr in the future. (Figs 2, 3, and 4.)

It is interesting to look at the predicted structure of the Sun at the present, in comparison with the range of data accessible to our current experimental platforms at NIF. (Figs 5, 6, and 7.)

Perturbations were made of a increase or decrease in stiffness of the EOS calculation, by global constant factor. The simulation of the evolution of the system was then repeated with the perturbed EOS. A percent change in the EOS produced a  $\sim 10\%$  change in the lifetime, considered as the time from formation to expansion as a red giant. A softer EOS led to a shorter lifetime, as one would expect as the compression at the center would then be greater and hence the rate of thermonuclear reactions higher. (Fig. 8.)

These simulations also illustrate the significance of the raw sensitivity: with a perturbed EOS, the radius and luminosity at  $\sim 4.5$  Gyr are different than observed for the Sun. Since the age of the Sun can be estimated or constrained in other ways, such as by isotopic abundances, it would be necessary to compensate for a perturbation in the EOS by adjusting other aspects of the model, such as the elemental abundances or transport properties. If these other properties are themselves constrained in other ways, the simulated evolution of the Sun may be used as a constraint on the EOS, if the underlying assumptions, observations, and chain of reasoning can be defined precisely enough.

From the simulations, a representative state at the center of the Sun around the present is 62% by mass He and 2% higher Z elements, the rest being H, with a mass density of  $162.2\text{g/cm}^3$  and a temperature of  $1.35\text{keV}$ . It is interesting to compare the variations between general-purpose EOS at these conditions. EOS are constructed for a fixed composition of matter. Unless an EOS has been constructed for a specific composition of interest, or as a function of composition such that the EOS for the specific composition can be obtained by interpolation, then a mixture model is used to estimate the EOS from endpoints of widely-varying composition, such as for the component elements. For a direct comparison of common EOS, we compare EOS for the same composition at the density and temperature state of the center, without adjusting the mass den-

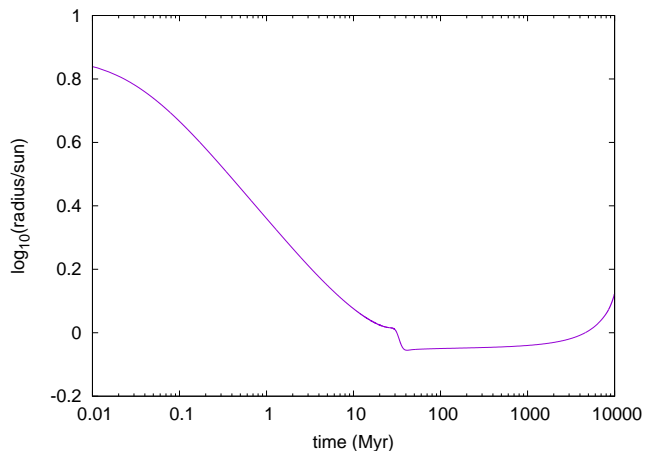


Fig. 1.— Evolution of a star of the mass of the Sun, logarithmic time scale showing early contraction.

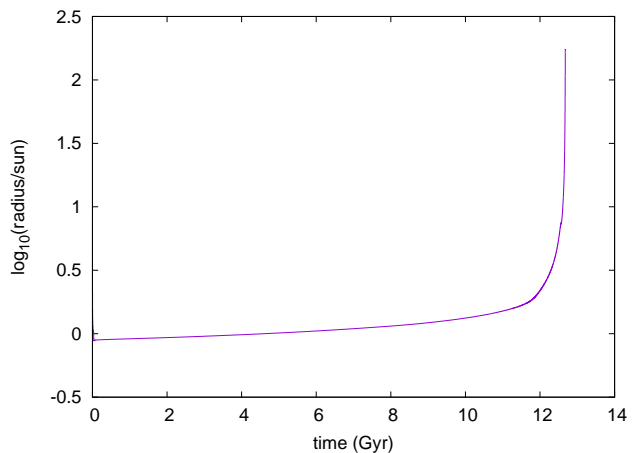


Fig. 2.— Evolution of the radius of the Sun in the baseline simulation.

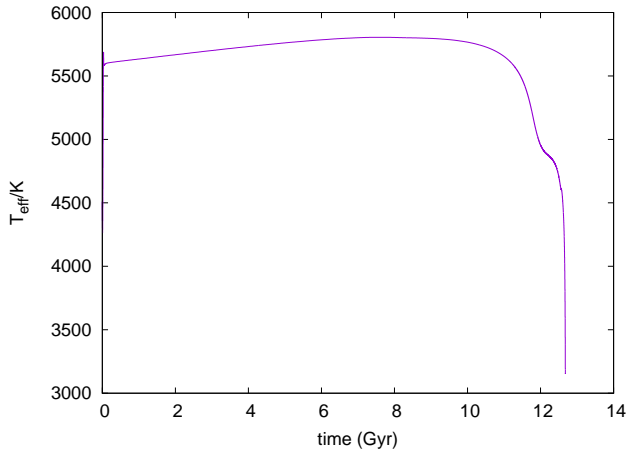


Fig. 3.— Evolution of the effective temperature of the Sun in the baseline simulation.

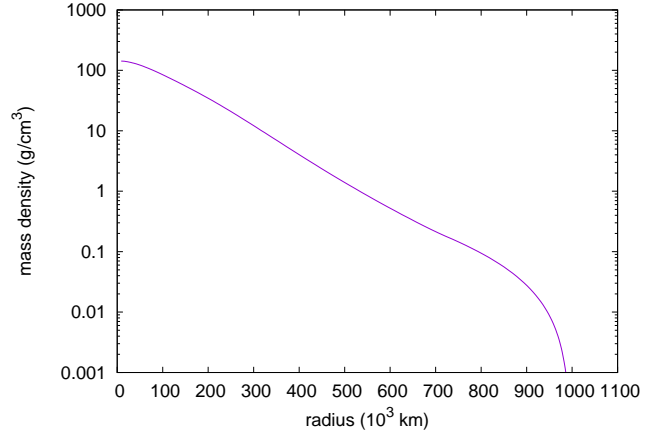


Fig. 5.— Mass density profile through the Sun in the baseline simulation at 4.6 Gyr.

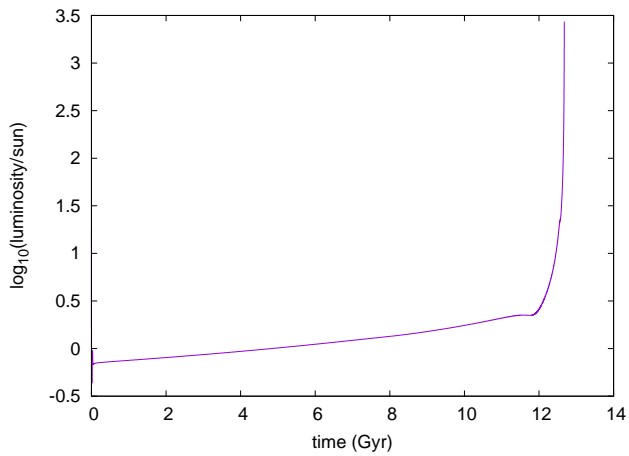


Fig. 4.— Evolution of the luminosity of the Sun in the baseline simulation.

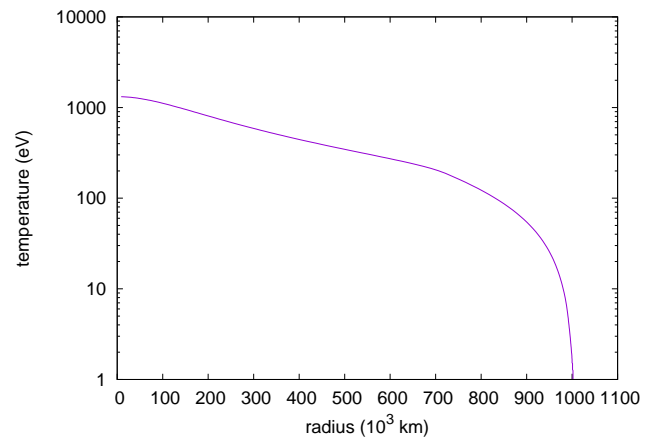


Fig. 6.— Temperature profile through the Sun in the baseline simulation at 4.6 Gyr.

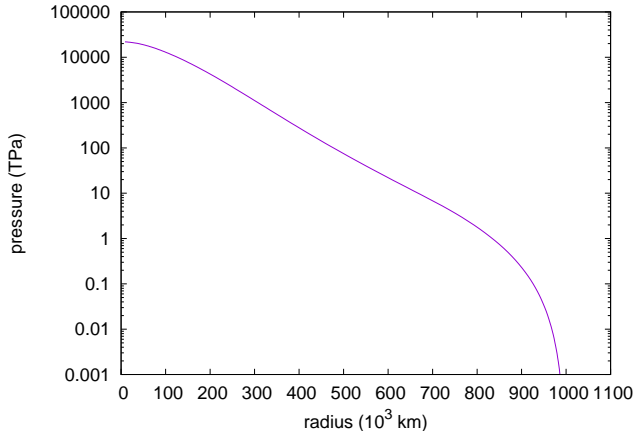


Fig. 7.— Pressure profile through the Sun in the baseline simulation at 4.6 Gyr.

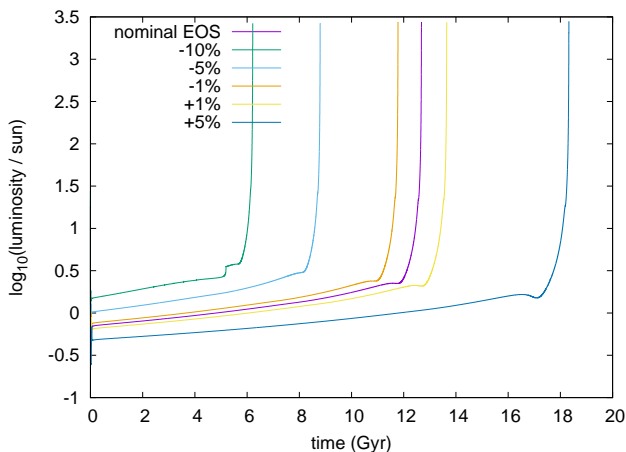


Fig. 8.— Sensitivity of the life of the Sun to variations in the equation of state.

sity for composition. EOS were taken from the Los Alamos National Laboratory SESAME library Holian (1984); Lyon & Johnson (1992) and the Lawrence Livermore National Laboratory LEOS library More et al (1988); Young & Corey (1995), and also from calculations using a recent development of the atom-in-jellium (AJ) method Swift et al (2019), including mixture constructions for compositions matching the STARS prediction of the center of the Sun. Most wide-range EOS use Thomas-Fermi (TF) theory (Thomas 1927; Fermi 1927) for the electron-thermal energy, which dominates under these conditions. The AJ EOS were constructed using the INFERNO computer program, which includes alternative approaches for calculating the free energy Liberman (1979); Liberman & Bennett (1990). The difference between these models gives an indication of the model uncertainty, and so we list both. The SESAME library includes an EOS, 5280, for a composition relevant to the Sun: the Ross-Aller solar composition. (Table 1.)

It is interesting to see the difference between EOS constructed using essentially the same widely-used model (TF) by different operators and using different computer programs, even for an element: several tens of percent, for H. The TF and AJ EOS for He were much more consistent, though the variations still of the order of 1%, which equates to a significant difference with respect to the lifetime of the Sun. The TF-based EOS for Ross-Aller solar mixture was implausibly high in pressure. The EOS calculation in the STARS simulation was almost 20% softer than the AJ calculation, representing the best self-consistent EOS theory used here. Given the sensitivity of the lifetime of the Sun to the EOS, these differences are enormous, and illustrate the degree to which uncertainties in the EOS may be masked by making adjustments to transport calculations or thermonuclear cross-sections..

#### 4. Lower mass limit of a red dwarf

As discussed below, an important question is the uncertainty in the mass budget for exotic dark matter attributable to the EOS. Self-gravitating bodies can be collected into different populations, based on the source of mass and competing mechanisms for accretion and dispersal. These popu-

Table 1: Pressure from various equations of state for the conditions at the center of the Sun.

composition	model	pressure (PPa)
H	TF: LEOS 11	35.88
	TF: SESAME 5250, 5251	57.56, 42.09
	AJ	45.15, 45.28
He	TF: SESAME 5760, 5761	15.84, 15.93
	AJ	15.71, 15.61
H-21.4He-1.7O	TF with mixing: SESAME 5280	61.5
H-{62,64}He	AJ with mixing	27.02, 26.43
H-62He-2O	AJ with mixing	26.40
H-62He-2M	STARS	21.87

lations include the successive generations of stars, and also the (exo)planets that form from the residual matter following the accretion of each star. In each population, most mass is contained within the end of the distribution comprising smaller bodies. For the population of bodies accreting from stellar nebulae, the small-mass bodies are the brown dwarfs. Assessing the ratio of luminous to non-luminous mass in this population this depends on determining the lower mass limit for a brown dwarf to form and emit radiation by internal thermonuclear reactions.

However, brown dwarfs are thought to burn deuterium rather than hydrogen, and so are more sensitive to the composition of the nebula from which they form. Brown dwarfs are also dim and relatively difficult to observe. It is also more difficult to relate the luminosity uniquely and reliably to the mass, as they are thought to have dust in their atmosphere. We consider instead the lower mass limit of red dwarfs.

For red dwarfs, we performed simulations with different masses for the initial nebula, and found the minimum mass at which nuclear reactions impeded the gravitational collapse and led to a long-lived star. This scan over masses was repeated with perturbations to the EOS, to find the sensitivity of the minimum mass to the EOS. With the default EOS, the lower mass limit of a red dwarf was calculated to be  $0.067 M_{\text{Sun}}$ , consistent with the accepted value. With an EOS perturbed to be 10% softer, the lower mass limit was calculated to be  $0.063 M_{\text{Sun}}$ :  $\sim 7\%$  less. However, the lower luminosity limit rose from  $-3.6$  to  $-3.2$  (logarithm to base 10), i.e. a factor 2.52 greater. (Fig. 9.)

From the simulations, a representative state at

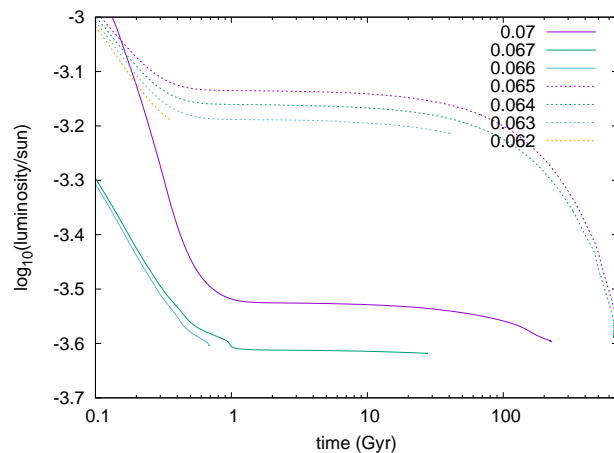


Fig. 9.— Sensitivity of red dwarf lighting to variations in the equation of state. Each curve represents a simulation with a different initial mass, as a fraction of that of the Sun. The solid lines are simulations with the baseline EOS; the dashed lines for EOS reduced by 10%.

the center of a minimum mass red dwarf is 28% by mass He and 2% higher Z elements, the rest being H, with a mass density of  $410.2 \text{ g/cm}^3$  and a temperature of 234 eV. (Table 2.)

In the cooler, denser conditions at the center of a red dwarf, the TF EOS varied over a narrower range than for the conditions at the center of the Sun. The difference between TF and AJ for He was an order of magnitude greater. The EOS calculation in the STARS simulation was 40% stiffer than the AJ calculation, a striking reversal in comparison with the case of the Sun. These differences are significant with respect to the sensitivity of the lower mass limit of a red dwarf to the EOS, and are absolutely dominant with respect to the sensitivity of the lower luminosity limit.

## 5. Mass budget for exotic dark matter

Dark matter was first postulated as an explanation for galactic rotation curves, most of which imply that more mass is present at outer radii than would be implied by the expected ratio of non-luminous matter to luminous matter in stars (for example, Ma et al (2014)). Current estimates of the discrepancy suggest that exotic dark matter must account for 85% of the matter in the universe, i.e. that the ratio of exotic dark matter to baryonic matter is  $\sim 5.7$ .

The ratio of non-luminous to luminous baryonic matter is estimated using models of the formation and evolution of stars and galaxies. The observational baryon census is non-trivial. For stars, a model is needed to convert the absolute magnitude to mass. This model depends on stellar structure theory, and thus on the EOS. Observational calibrations of the relationship have significant uncertainty, especially at low mass (Armitage & Clark 1996).

As mentioned above, bodies condensing from a nebula are expected to follow a power-law distribution which must cut off at low mass. However, this cut-off is poorly understood; this is important as most of the total mass occurs in low-mass objects. In contrast, the luminosity of a galaxy is dominated by massive, short-lived stars; these are also poorly understood. The total baryonic mass is correlated with models of baryogenesis in the Big Bang, and of galactic evolution.

If the mass distribution has the form  $\xi_0 M^{-\alpha}$ ,

then the ratio of total to baryonic mass varies as  $M^{\alpha-1}$ . Salpeter's estimate of the mass distribution was  $\alpha \simeq 2.35$  (Salpeter 1955). Using the sensitivity of red dwarf mass limit to EOS, the uncertainty in baryonic mass is at least 30%, i.e. at least 5% in exotic dark matter. Using the sensitivity of the red dwarf luminosity limit, the uncertainty in EOS dominates, contributing tens of percent to the uncertainty in exotic dark matter.

## 6. Conclusions

Simulations of stellar formation and evolution are very sensitive to the equation of state of stellar matter. The lifetime of the Sun changes by  $\sim 10\%$  for a 1% change in the EOS. The threshold mass for red dwarf ignition is less sensitive to the EOS, changing by  $\sim 7\%$  for a 10% change in the EOS, but the luminosity at the threshold is significantly more sensitive, varying by  $\sim 250\%$ . The ratio of luminous to non-luminous matter in the galaxy is likely to be at least as sensitive. Relevant EOS are uncertain at the  $\sim 10\%$  level for the Sun and  $\sim 30\%$  for red or brown dwarfs. Compared to the models used in the STARS program, the best mixture EOS currently available suggest a pressure  $\sim 20\%$  greater for representative conditions at the center of the Sun, and  $\sim 25\%$  for corresponding conditions in a red dwarf. These sensitivities are greater than the net uncertainty from observational constraints, particularly of the Sun but also of red dwarfs, suggesting that astrophysical observations may provide a constraint on the EOS of stellar matter as well as on models of opacity and convection. It would also be worthwhile investigating a wider range of stellar structure calculations using more accurate EOS models.

## Acknowledgments

This work was performed under the auspices of the U.S. Department of Energy under contract DE-AC52-07NA27344.

## REFERENCES

- Albers, R. & Johnson, J.D. 1982, documentation for SESAME EOS 5251 for H, in Holian (1984)
- Alexander, D.R., & Ferguson, J.W. 1994, ApJ, 437, 879

Table 2: Pressure from various equations of state for the conditions at the center of a minimum mass red dwarf.

composition	model	pressure (PPa)
H	TF: LEOS 11	27.88
	TF: SESAME 5250, 5251	25.19, 33.86
	AJ	22.34, 22.18
He	TF: SESAME 5760, 5761	9.94, 10.39
	AJ	8.22, 8.18
H-21.4He-1.7O	TF with mixing: SESAME 5280	14.12
H-{62,64}He	AJ with mixing	18.42, 18.14
H-62He-2O	AJ with mixing	18.24
H-62He-2M	STARS	25.55

- Armitage, P., & C. Clarke, C. 1996, MNRAS 280, 458
- Döppner, T., Swift, D.C., Kritcher, A.L., Bachmann, B., Collins, G.W., Chapman, D.A., Hawreliak, J., Kraus, D., Nilsen, J., Rothman, S., Benedict, L.X., Dewald, E., Fratanduono, D.E., Gaffney, J.A., Glenzer, S.H., Hamel, S., Landen, O.L., Lee, H.-J., LePape, S., Ma, T., MacDonald, M.J., MacPhee, A.G., Milathianaki, D., Millot, M., Neumayer, P., Sterne, P.A., Tommasini, R., & Falcone, R.W. 2018, Phys. Rev. Lett., 121, 025001
- Eggleton, P.P. 1971 MNRAS, 151, 351
- Eggleton, P.P. 1972 MNRAS, 156, 361
- Eggleton, P.P. 1973 MNRAS, 163, 279
- Eggleton, P.P. Faulkner, J., Flannery B. P. 1973, A&A, 23, 325
- Eldridge, J.J., & Tout, C. A. 2004, MNRAS, 348, 201
- Fermi, E. 1927, Rend. Accad. Naz. Lincei., 6, 602607
- Guzik, J.A., Fontes, C.J., & Fryer, C 2018, arXiv:1806.06743
- Holian, K.S. (Ed.) 1984, Los Alamos National Laboratory report LA-10160-MS Vol 1c
- Iglesias, C.A., Rogers, F.J., & Wilson, B.G. 1992, ApJ, 397, 717
- Itoh, N., & Kohyama, Y. 1983, ApJ, 275, 858
- Itoh, N., Mitake, S., Iyetomi, H., & Ichimaru, S. 1983, ApJ, 273, 774
- Itoh, N., Adachi, T., Nakagawa, M., Kohyama, Y., & Munakata, H. 1989, ApJ, 339, 354 (erratum 360, 741)
- Itoh, N., Mutoh, H., Hikita, A., & Kohyama, Y., H. 1992, ApJ, 395, 622 (erratum 404, 418)
- Keeley, D.A. 1970, ApJ, 161, 643
- Kritcher, A.L., Swift, D.C., Döppner, T., Bachmann, B., Benedict, L.X., Collins, G.W., DuBois, J.L., Elsner, F., Fontaine, G., Gaffney, J.A., Hamel, S., Jenei, A., Johnson, W.R., Kostinski, N., Kraus, D., MacDonald, M., Maddox, B., Martin, M.E., Neumayer, P., Nikroo, A., Nilsen, J., Remington, B.A., Saumon, D., Sterne, P.A., Sweet, W., Correa Tedesco, A.A., Whitley, H.D., Falcone, R.W., Glenzer, S.H. 2020 Nature (in press)
- Liberman, D.A. 1979, Phys. Rev. B, 20, 12, 4981
- Liberman, D.A. & Bennett, B.I. 1990, Phys. Rev. B, 42, 2475
- Lyon, S.P. & Johnson, J.D. 1992, Los Alamos National Laboratory report LA-UR-92-3407
- Ma, C.-P., Greene, J.E., Murphy, J.D., McConnell, N., Janish, R., Blakeslee, J.P., & Thomas, J. 2014, ApJ, 795, 2, 158
- Marigo, P. 2002, A&A, 387, 507
- More, R.M., Warren, K.H., Young, D.A. and Zimmerman, G.B. 1988, Phys. Fluids, 31, 3059



- Pols, O.R., Tout, C.A., Eggleton, P. P., & Han Z. 1995, MNRAS, 274, 964
- Rossi, S.C.F. & Maciel, W.J. 1983 Astrophys Space Sci, 96, 205
- Salpeter, E.E. 1955, ApJ, 121, 161
- Scalo, J.M. & Ulrich, R.K. 1975 Apl, 183, 151
- Schroeder, K.P., Pols, O. R., & Eggleton, P.P. 1997, MNRAS, 285, 696
- Stancliffe, R.J., & Eldridge, J.J. 2009, MNRAS, 396, 1699
- Stancliffe, R.J., Tout, C.A., & Pols, O.R. 2004, MNRAS, 352, 984
- Stancliffe, R.J., Lugaro, M., Ugalde, C., Tout, C.A., Goerres, J., & Wiescher, M. 2005, MNRAS, 360, 375
- Stancliffe, R.J., Glebbeek, E., Izzard, R.G., & Pols, O.R. 2007, A&A, 464, L57
- Swift, D.C., Kritcher, A.L., Hawreliak, J.A., Lazicki, A., MacPhee, A., Bachmann, B., Döppner, T., Nilsen, J., Collins, G.W., Glenzer, S., Rothman, S.D., Kraus, D., & Falcone, R.W. 2018, Rev. Sci. Instrum., 89, 053505
- Swift, D.C., Lockard, T., Kraus, R.G., Benedict, L.X., Sterne, P.A., Bethkenhagen, M., Hamel, S., & Bennett, B.I. 2019, Phys. Rev. E, 99, 063210
- Swift, D.C., Kritcher, A.L., Hawreliak, J.A., Gaffney, J., Lazicki, A., MacPhee, A., Bachmann, B., Döppner, T., Nilsen, J., Whitley, H.D., Collins, G.W., Glenzer, S., Rothman, S.D., Kraus, D., & Falcone, R.W. 2020, submitted and [arXiv:2006.13342](https://arxiv.org/abs/2006.13342)
- Thomas, L.H. 1927, Proc. Cambridge Phil. Soc., 23, 5, 542548
- Vardya, M.S. 1960 ApJS, 4, 281
- Webbink, R.F. 1975 PhD thesis, Univ. of Cambridge
- Young, D.A., & Corey, E.M. 1995, J. Appl. Phys., 78, 3748